

Geochemical Rate-RNA Integration Study: Ribulose-1,5-Bisphosphate Carboxylase/Oxygenase Gene Transcription and Photosynthetic Capacity of Planktonic Photoautotrophs

Jorge E. Corredor,¹ Boris Wawrik,² John H. Paul,² Hiep Tran,³
Lee Kerkhof,^{3*} José M. López,¹ Angel Dieppa,¹
and Oswaldo Cárdenas¹

*Department of Marine Sciences, University of Puerto Rico, Lajas, Puerto Rico¹;
College of Marine Science, University of South Florida, St. Petersburg, Florida²;
and Institute of Marine and Coastal Sciences, Rutgers University,
New Brunswick, New Jersey³*

Received 15 October 2003/Accepted 5 May 2004

A pilot field experiment to assess the relationship between traditional biogeochemical rate measurements and transcriptional activity of microbial populations was carried out at the LEO 15 site off Tuckerton, N.J. Here, we report the relationship between photosynthetic capacity of autotrophic plankton and transcriptional activity of the large subunit gene (*rbcL*) for ribulose-1,5-bisphosphate carboxylase/oxygenase (RubisCO), the enzyme responsible for primary carbon fixation during photosynthesis. Similar diel patterns of carbon fixation and *rbcL* gene expression were observed in three of four time series, with maxima for photosynthetic capacity (P_{\max}) and *rbcL* mRNA occurring between 10 a.m. and 1 p.m.. The lowest P_{\max} and *rbcL* levels were detected between 6 p.m. and 10:30 p.m.. A significant correlation was found between P_{\max} and form ID *rbcL* mRNA ($R^2 = 0.56$) and forms IA and IB ($R^2 = 0.41$ and 0.47 , respectively). The correlation between the abundance of “diatom” *rbcL* and P_{\max} mRNA was modest ($R^2 = 0.49$; $n = 12$) but improved dramatically ($R^2 = 0.97$; $n = 10$) upon removal of two outliers which represented afternoon samples with high P_{\max} but lower mRNA levels. Clone libraries from reverse transcription-PCR-amplified *rbcL* mRNA indicated the presence of several chromophytic algae (diatoms, prymnesiophytes, and chrysophytes) and some eukaryotic green flagellates. Analogous results were obtained from amplified small rRNA sequences and secondary pigment analysis. These results suggest that diatoms were a major contributor to carbon fixation at LEO 15 at the time of sampling and that photosynthetic carbon fixation was partially controlled by transcriptional regulation of the RubisCO gene.

A primary research goal for marine environmental biogeochemistry is a thorough understanding of the molecular to global scale links and feedback mechanisms between solar irradiance, marine microbial activity, primary productivity, carbon and nitrogen cycles, and remotely sensed ocean color data. Increased emphasis is now being placed on the application of modern molecular tools to address these problems. Understanding of the genetic basis of biogeochemical processes and, more importantly, the expression of relevant genes in the marine environment is perceived as a promising route to these goals. A detailed understanding of the connection between gene expression, protein translation, and enzyme activity in environmental systems can provide significant insight into the mechanisms controlling biogeochemical transformation rates.

To this end, a pilot field experiment was carried out to test whether mRNA levels from complex, indigenous phytoplankton and bacterial populations can be related to biogeochemical rate processes mediated by these communities. The Geochemical Rate-RNA Integration Study (GRIST) incorporated several different biogeochemical measurements and molecular ap-

proaches (6). The experiment was designed to provide guiding principles on how the combination of the flux determinations and the quantification of microbial transcriptional activity can be used to better understand the regulation and response of microbial activity to different environmental parameters. Measurements have focused on C and N cycling and included primary production, bacterial production, dissolved organic matter production and uptake, inorganic and organic N assimilation, and N redox cycling in water column and sediment samples.

Concurrently, a suite of molecular approaches were used to quantify gene product abundance over two diel cycles. We employed partial-length gene probes to identify the major clades of *rbcL* mRNA in oceanic phytoplankton (13, 18, 23). Form IA *rbcL* is found in phycoerythrin-containing picocyanobacteria such as *Synechococcus* as well as *Prochlorococcus*. Form IB *rbcL* is found in chlorophytes and certain picocyanobacteria, whereas form ID of the enzyme is found in chromophytic phytoplankton (diatoms, prymnesiophytes, pelagophytes, bolidophytes, rhodophytes, chrysophytes, and some dinoflagellates) (22, 23). We here report on the relationship between the photosynthetic capacity of autotrophic plankton and the transcriptional activity of variants of the large subunit gene (*rbcL*) for ribulose-1,5-bisphosphate carboxylase/oxygen-

* Corresponding author. Mailing address: Institute of Marine and Coastal Sciences, Rutgers University, New Brunswick, NJ 08901. Phone: (732) 932-6555, ext. 335. Fax: (732) 932-6520. E-mail: kerkhof@imcs.rutgers.edu.

ase (RubisCO), the enzyme in the first step of the Calvin-Benson-Bassham pathway of autotrophic carbon fixation (21).

MATERIALS AND METHODS

The GRIST experiment was carried out at the Rutgers University Marine Field Station at Tuckerton, N.J. (19 to 25 July 2002). Sampling was carried out at the well-characterized Long-Term Ecosystem Observatory (4). Diel periodicity was explored at 4-h intervals over two daily cycles (20 July 2002 and 22 July 2002), referred to hereafter as day 1 and day 2, respectively. Filtration for biogeochemical and molecular analyses occurred at sea aboard the R/V *Arabella*, and samples were flash-frozen on deck, either on dry ice or in liquid N₂.

Photosynthetic pigments and elemental analysis. Chlorophyll *a* concentration of GF/F-filtered samples was determined fluorometrically after 90% acetone extraction with the method of Welschmeyer (25). High-pressure liquid chromatographic analysis of photosynthetic pigments was carried out following the procedure described by Wright et al. (26) with a C₁₈ Waters Symmetry column (3.9 by 150 mm) on a Shimadzu LC-10AT instrument equipped with an SPD-M10AV diode array detector. The high-pressure liquid chromatograph was calibrated with a pure (Sigma Chemical) chlorophyll *a* solution in 90% acetone. To increase resolution and allow separation of zeaxanthin from lutein, the mobile-phase program was modified as follows: 0 to 4 min, 1 ml min⁻¹, B (90:10 methanol-0.5 M aqueous ammonium acetate, pH 7.2, vol/vol), ramp to C (90:10 acetonitrile-water, vol/vol); 4 to 5.5 min, increase flow to 1.8 ml min⁻¹, 4 to 18 min, ramp to 20% C, 80% D (ethyl acetate); 18 to 21 min, 1 ml min⁻¹ ramp to C; 21 to 24 min, ramp C to B for restart. Particulate organic C and N content was determined with a CE Elantech CHN elemental analyzer.

Photosynthetic parameters. Water samples for experimental determination of phytoplankton photosynthetic capacity representative of surface and bottom (14 m) assemblages were transported to the dockside laboratory at the Rutgers University Marine Field Station (<45-min transit time). Samples were transferred to 1-liter light-shielded, acid-washed polyethylene bottles, of which a 650-ml subsample was spiked with 0.108 mCi of [¹⁴C]bicarbonate (Amersham Pharmacia Biotech) for a 0.167-μCi initial activity. Aliquots (40 ml) of the spiked water were transferred to 40-ml borosilicate Environmental Protection Agency vials and incubated for 2 h in a photosynthetron apparatus (CHPT Mfg Co.) at constant temperature (17°C) and irradiances ranging from 0 (dark sample) to 614 μE m⁻² s⁻¹. A time-zero sample blank was immediately filtered prior to commencement of incubation. Following incubation, samples were filtered onto 25-cm GF/F glass fiber filters and treated with 250 μl of 10% HCl to drive off unfixed [¹⁴C]bicarbonate. After 24 h, 10 ml of BCS scintillation fluid (Amersham Pharmacia Biotech) were added, and sample radioactivity was determined on a Beckman L6000 liquid scintillation counter with the channels ratio mode. The resulting data were plotted in *P* versus *E* (irradiance) curves, and the photosynthetic parameters α (response to low light), P^B_{max} (photosynthetic capacity normalized to chlorophyll *a* content), and β (susceptibility to photoinhibition) were computed with the exponential formulation of Platt et al. (20).

***rbcL* mRNA analysis by probe hybridization.** mRNA was extracted from seawater with RNeasy spin columns (QIAGEN) as previously described (12). Briefly, either 100- or 200-ml seawater samples were treated with 0.1% diethylpyrocarbonate (Sigma Chemical Corp.) and filtered onto 25-mm, 0.45-μm HV polyvinylidene difluoride filters (Millipore Durapore). Filters were stored in liquid nitrogen in 750 μl of RLT lysis buffer (QIAGEN) together with 0.2 g of baked glass beads (Biospec Products). Cell lysis was achieved by bead beating; 500 μl of lysate was then extracted following the RNeasy kit (QIAGEN) protocol. Samples were split three ways. One third was digested with DNase-free RNase (Promega, Madison, Wis.), and one third was digested with RQ1 DNase (Promega). RNA was then immobilized onto Zeta-Probe charged nylon filters (Bio-Rad) by dot blotting and UV cross-linking. Duplicate samples were probed with form IA, form IB, and form ID *rbcL* probes previously described (7, 16). [³⁵S]UTP-labeled probes were prepared by *in vitro* transcription. Dot blots were analyzed with a Bio-Rad model GS363 molecular imager. Standard curves were made from opposite orientation *in vitro* transcripts generated from the same *rbcL* clones used to make the riboprobes.

To detect the proportion of form ID hybridization signal by diatoms, a quantitative PCR assay was performed. Samples were filtered as above but the diethylpyrocarbonate treatment was omitted. Aliquots of the RNeasy eluates were amplified as described with chromophytic *rbcL* primers and a diatom-specific TaqMan probe (24).

Extraction of mRNA and rRNA for RT-PCR. Two methods were used to obtain *rbcL* mRNA and intact ribosomes. For mRNA analyses, 200 ml of seawater was filtered from the 2:00 p.m. sample of the surface water from the first diel and filters were stored in 750 μl of RLT (QIAGEN) and stored in liquid

nitrogen. Samples were not treated with diethylpyrocarbonate, if they were intended for reverse transcription (RT)-PCRs. Upon extraction samples were DNase digested on the RNeasy columns for 15 min with the RNase-free DNase reagent set (QIAGEN) according to the protocol provided by QIAGEN.

Reverse transcriptions were performed with random hexamers, 4.7 mM MgCl₂, and Moloney murine leukemia virus reverse transcriptase (Promega) for 30 min at 37°C and freshly extracted RNA; 5 μl was then added to a PCR. Two primer sets were used to amplify the *rbcL* fragments. The form IA/B primer set produced a 615-bp fragment (forward primer: 5'-TCIGCITGRAACTAYGGTCG-3'; reverse primer: 5'-CTGAGIGGIAARAACACGG-3') and the form ID set produced a 554-bp fragment (forward primer: 5'-GATGATGARAAYATTA CTC-3'; reverse primer: 5'-ATTGDCACAGTGDATACCA-3'). All sequences are stated with International Union of Pure and Applied Chemistry (IUPAC) degeneracy. PCR conditions were as follows: 1 μM final concentration for both primers, 1.5 mM MgCl₂, 2.5 mM each nucleotide, and 5 U of *Taq* polymerase (Promega). Cycle parameters were 3 min at 95°C, followed by 40 cycles of 1 min at 95°C, 1 min at 52°C, and 1 min 30 sec at 72°C. Cycling was followed by a 15-min 72°C elongation step.

For intact ribosome extraction from phytoplankton, a modified phenol-chloroform procedure incorporating multiple freeze-thaw cycles was used as described previously (7). Total nucleic acid pellets were resuspended in diethylpyrocarbonate-treated water, and the ribosomal small subunit was gel purified with an RNaid kit (Bio 101, Carlsbad, Calif.). The purified small subunit was diluted 10⁻⁵ to 10⁻⁶ and used as a template in an RT-PCR with an 18S rRNA eukaryotic forward primer (5'-ACC TGG TTG ATC CTG CCA G-3') and a universal reverse primer (519R; 5'-ATTACC GCG GCT GCT GG-3') with the Titan RT-PCR kit (Roche) containing the RNase inhibitor anti-RNase (Ambion). The cycling parameters were 50°C for 30 min, 94°C for 2.5 min, 25 cycles of 94°C for 1 min, 55°C for 2 min, and 72°C for 3.5 min, followed by a final extension at 72°C for 10 min.

Clone libraries. *rbcL* genes from mRNA were RT-PCR amplified from one sampling time with the primer sets described above. Immediately after amplification, products were purified with the Quiaquick PCR purification kit (QIAGEN) or with a GeneClean kit (Bio 101). Amplicons were ligated into the PCR II vector with a TA dual promoter cloning kit (Invitrogen). RubisCO clones were screened for the correct insert size by PCR and for unique restriction patterns with *Sau3AI* and *AluI* before sequencing in an Applied Biosystems model 373 sequencer by the University of Florida core sequencing laboratory (University of Florida, Gainesville, Fla.). rRNA clones were obtained from both surface and bottom samples during day 2. Clones were screened by terminal restriction fragment length polymorphism analysis by digestion with *MspI*, and selected clones were sequenced on an ABI 310 as described previously (8).

Phylogenetic analysis. RubisCO cDNA sequences were translated into amino acids and aligned with their closest match found in GenBank as determined by BLAST searching as well as sequences we previously recovered from similar environments (14, 23). Alignment was performed with Omega 1.1 (Oxford Molecular Group, Oxford, United Kingdom) with a ClustalW pairwise weighted alignment method. Amino acid sequences were used to avoid potential biases introduced by codon usage and GC content. Alignments were inspected for obvious misalignments and exported to Mega 2.0 beta (10). Trees were built with both parsimony and the neighbor-joining method with a gamma distribution (gamma parameter = 2.0) to correct for rate heterogeneity across sites. rRNA genes were initially aligned with ClustalW and later aligned by hand. Phylogenetic trees were reconstructed by maximum-likelihood methods with fastDNAML.

Nucleotide sequence accession number. Accession numbers for the RubisCO clones are AY356325 to AY356346. Accession numbers for the 18S rRNA clones are AY378156 to AY378164.

RESULTS

Water mass properties varied moderately during the experiment, with initial surface temperatures of 19°C increasing to 22°C during day 1 (Fig. 1). Day 2 surface waters increased in temperature from 22 to 24°C by the end of the experiment. Deeper water also experienced slight warming from 16 to 17°C, with upper layer stratification being apparent. Practical salinity during the sample period ranged from 31.6 (surface) to 32 (deep), with an increase of less than 0.2 in surface water at the 19:00 and 22:00 time points of day 2 (data not shown). An additional intrusion of warmer water at the sample site was also evident between 6 and 10 a.m. during day 1 at approxi-

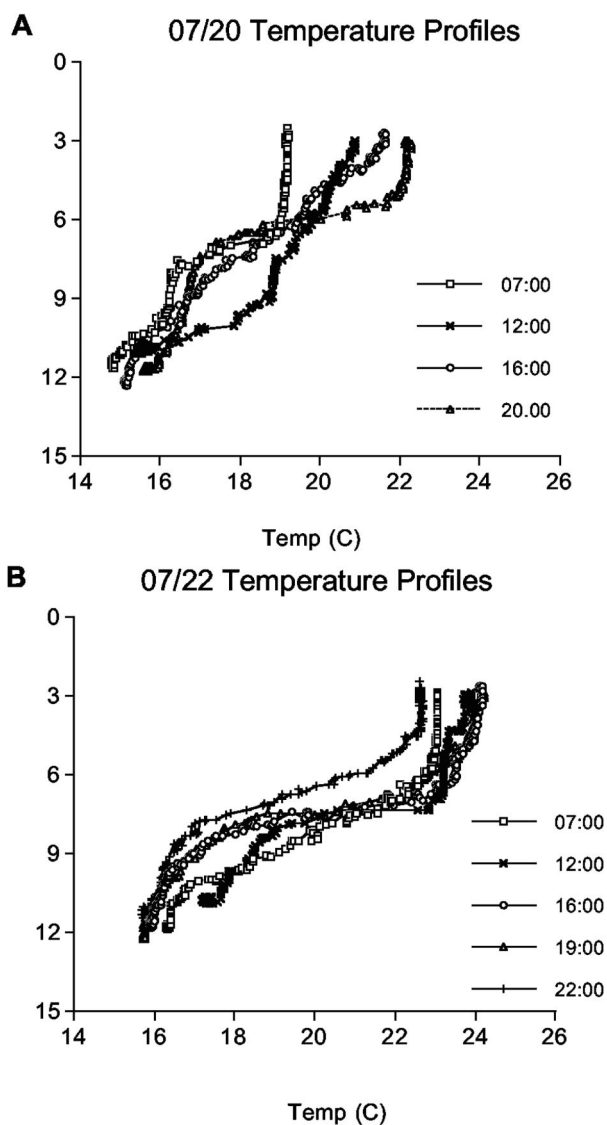


FIG. 1. Temperature versus depth data for day 1 (A) and day 2 (B).

mately 12:00. However, no samples for primary production, *rbcL* mRNA, or 18S rRNA were collected at these intermediate depths during the experiments.

Surface chlorophyll *a*, particulate organic C, and particulate organic N concentrations all increased from approximately 18:00 on day 1 to 19:00 on day 2, suggesting that a small phytoplankton bloom was under way (Fig. 2). The chlorophyll *a* concentration ranged between 3 and 16 mg m⁻³ during day 1 and between 2.6 and 34.7 mg m⁻³ during day 2 with deep water (14 m) chlorophyll *a* variation substantially lower than surface variation. Particulate organic C concentrations varied between 0.48 and 3.2 mg liter⁻¹ and particulate organic N concentrations ranged between 0.08 and 0.49 mg liter⁻¹ (Fig. 2). Both particulate organic C ($r^2 = 0.86$) and particulate organic N ($r^2 = 0.90$) were significantly correlated to chlorophyll *a* and for the most part followed a temporal pattern similar to that observed for chlorophyll *a*. Chlorophyll *a*, particulate organic C, and particulate organic N content were

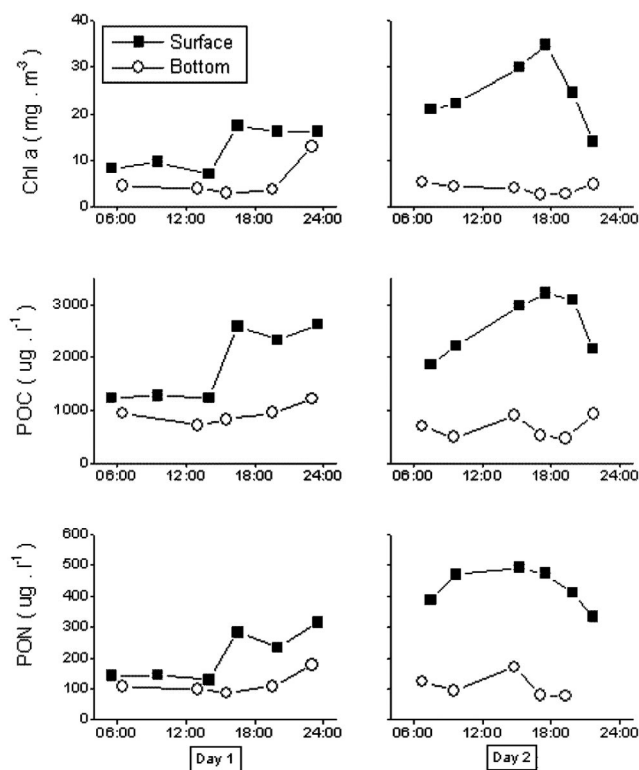


FIG. 2. Time course for chlorophyll *a* (Chl *a*), particulate organic C (POC), and particulate organic N (PON) at the LEO 15 node A site.

consistently greater near the surface than at depth during the course of the experiment.

Relative to the Redfield C:N ratio of 7.1, surface particulate organic matter (8.8) was significantly depleted in N, while particulate organic matter at depth (5.9) was N rich. These differences may reflect enhanced pigment and protein synthesis in light-limited deep waters relative to greater carbohydrate and lipid synthesis in surface waters. Chlorophyll *a* values, as determined by HPLC, were about 65% of those reported by bulk fluorometry, indicating positive interference by other chlorophylls in the fluorometric method. Chlorophyll *a* was the dominant photosynthetic pigment. Fucoxanthin was the dominant accessory pigment representing 28% of the total chlorophyll *a*, followed by chlorophyll *b* (15% chlorophyll *a*). Fucoxanthin was significantly correlated with chlorophyll *a* ($r^2 = 0.52$, $P < 0.01$). Other pigments present in minor concentrations (<10% chlorophyll *a*) were, in order of abundance, chlorophyll *c*₂, zeaxanthin, peridinin, and chlorophyll *c*₁ (Table 1).

Surface photosynthetic rates during the first day were only measured during the initial hours of the experiment when chlorophyll *a* variability was low. Light-saturated photosynthetic rates (P_{max}), the maximum achievable C fixation rates, varied little in these samples, as was the case for deep-water samples despite a greater range in phytoplankton abundance, as reflected by chlorophyll *a*, particulate organic C, and particulate organic N content. During the second diel experiment, P_{max} varied substantially (Fig. 3, Table 2).

Photosynthetic capacity (P^B_{max}), the maximum achievable photosynthetic rate normalized to chlorophyll *a* concentration, ranged between 1.1 and 11.6 mg of C (mg of chlorophyll *a*)⁻¹

TABLE 1. Concentration of photosynthetic pigments at LEO 15 during the GRIST experiment as determined by HPLC

| Day | Depth | Time | Concn ($\mu\text{g/liter}$) | | | | | | | |
|--------|---------|-------|-------------------------------|----------------------|-----------------------------------|-----------------------------------|-----------|-------------|------------|------|
| | | | Chlorophyll <i>a</i> | Chlorophyll <i>b</i> | Chlorophyll <i>c</i> ₁ | Chlorophyll <i>c</i> ₂ | Peridinin | Fucoxanthin | Zeaxanthin | |
| 1 | Surface | 5:30 | 3.93 | 0.51 | 0.11 | 0.29 | 0.00 | 1.87 | 0.27 | |
| | | 9:30 | 5.83 | 1.26 | 0.09 | 0.28 | 0.01 | 0.45 | 0.26 | |
| | | 14:00 | 2.66 | 0.65 | 0.06 | 0.22 | 0.00 | 0.26 | 0.21 | |
| | | 16:30 | 7.81 | 1.32 | 0.20 | 0.66 | 0.04 | 4.03 | 0.68 | |
| | | 20:00 | 7.71 | 0.80 | 0.15 | 0.59 | 0.00 | 4.57 | 0.57 | |
| | | 23:30 | 11.81 | 1.34 | 0.32 | 0.83 | 0.00 | 7.20 | 0.82 | |
| | Bottom | 6:30 | 2.13 | 0.12 | 0.00 | 0.11 | 0.00 | 0.12 | 0.00 | |
| | | 13:00 | 2.09 | 0.15 | 0.00 | 0.13 | 0.00 | 0.25 | 0.00 | |
| | | 15:30 | 1.02 | 0.09 | 0.00 | 0.36 | 0.00 | 0.97 | 0.00 | |
| | | 19:30 | 1.59 | 0.08 | 0.00 | 0.10 | 0.00 | 1.55 | 0.00 | |
| | | 23:00 | | 1.15 | 0.14 | 0.60 | 0.00 | 2.92 | 0.43 | |
| | | 2 | Surface | 7:30 | 15.19 | 1.97 | 0.13 | 0.83 | 0.75 | 1.53 |
| | 9:40 | 16.61 | | 3.57 | 0.12 | 0.98 | 0.30 | 5.90 | 0.75 | |
| | 15:15 | 24.76 | | 5.29 | 0.06 | 1.17 | 0.38 | 4.64 | 0.25 | |
| 17:30 | 21.12 | 3.47 | | 0.11 | 1.19 | 0.17 | 4.42 | 0.39 | | |
| 19:50 | 11.15 | 1.67 | | 0.09 | 0.76 | 0.68 | 1.25 | 0.00 | | |
| 21:40 | 7.95 | 0.96 | | 0.09 | 0.74 | 0.10 | 2.05 | 0.00 | | |
| Bottom | 6:45 | 3.03 | | 0.12 | 0.00 | 0.14 | 0.00 | 0.28 | 0.00 | |
| | 9:30 | 2.88 | | 0.18 | 0.00 | 0.14 | 0.00 | 0.43 | 0.00 | |
| | 14:45 | 2.37 | | 0.14 | 0.00 | 0.14 | 0.14 | 0.82 | 0.00 | |
| | 17:00 | 1.38 | | 0.08 | 0.00 | 0.08 | 0.00 | 0.93 | 0.00 | |
| | 19:15 | 0.90 | 0.00 | 0.00 | 0.04 | 0.00 | 0.09 | 0.00 | | |
| | 21:40 | 1.95 | 0.16 | 0.00 | 0.13 | 0.00 | 0.20 | 0.00 | | |

h^{-1} , well within the range of values reported previously for phytoplankton assemblages of temperate coastal marine waters (2). Average $P_{\text{max}}^{\text{B}}$ was moderately higher at depth (6.9 m) than near the surface (4.8 m). The response to irradiance at low light levels (α) ranged between 0.03 and 0.25 mg of C (mg of chlorophyll *a*)⁻¹ $\mu\text{E}^{-1} \text{m}^{-2}$ and was higher on average at depth (0.13) than near the surface (0.09). Photoinhibition was apparent only in deep-water samples.

In the surface waters, *rbcL* mRNA levels were highest either at the first-light sampling (dawn; day 1 surface waters) or at 10:30 a.m. (Fig. 4). In the subsurface, maximum transcription occurred at the 10:30 or 1 p.m. sampling. The minimum transcriptional activity occurred at about 7:00 p.m. in both surface and bottom samples. During the first diel in the surface samples, form ID *rbcL* mRNA was the most abundant form of *rbcL* mRNA during the morning peak in transcriptional activity (Fig. 4). During the other three diel samples (day 1 bottom water and both surface and bottom for day 2), diatom *rbcL* mRNA displayed the greatest dynamic range among the *rbcL* forms that we quantified.

Taking the average *rbcL* mRNA levels for the daylight hours for this group of samples indicated that diatom *rbcL* was significantly greater than form IA or form IB, but not different from form ID ($P = 0.046$). Figure 5 shows the daylight average *rbcL* levels for all four time series. Bottom samples both showed a distinct increase in transcript abundance at the last sampling, 10:30 p.m. to 11:00 p.m., which was also reflected in particulate organic C and $P_{\text{max}}^{\text{B}}$. All three forms of *rbcL* mRNA quantified by hybridization were significantly correlated to each other at the 1% confidence interval (A to B: $P = 0.001$, A to D: $P = 0.01$, B to D: $P = 0.001$). Form IB and form ID *rbcL* mRNAs were also significantly correlated with diatom

rbcL mRNA quantified by real-time PCR. Form IA was not ($P = 0.12$). P_{max} was significantly correlated with all forms of *rbcL* that we quantified (A: $P = 0.01$, B: $P = 0.005$, D: $P = 0.001$, diatom: $P = 0.007$; see Fig. 9). P_{max} was least well correlated to form IA *rbcL* ($R^2 = 0.41$). P_{max} exhibited progressively tighter correlation to form IB ($R^2 = 0.47$) and to form ID *rbcL* mRNA ($R^2 = 0.56$). The best predictor of P_{max} was the cumulative *rbcL* mRNA signal obtained by adding form IA, IB, and ID hybridization numbers ($R^2 = 0.58$).

Cloning and sequencing of *rbcL* mRNA from transcriptionally active phytoplankton yielded 22 unique *rbcL* clones (Fig. 6). Table 3 gives a list of all unique sequences detected and their closest relatives in GenBank as determined by BlastP analysis (1). Phylogenetic analysis suggested that 14 of these clones were of the form ID type and likely included four diatoms, four prymnesiophytes, four chrysophytes, a rhodophyte, and a deeply rooted sequence most closely related to *Oolithodiscus luteus*. The remaining eight clones were of the form IB type and included two flagellated chlorophytes related to *Pyramimonas*, one sequence closely related to *Bathycoccus*, and a small clade of deeply rooted forms. No picocyanobacterium-like sequences (i.e., *Synechococcus* or *Prochlorococcus*) were detected.

To test whether diatoms, prymnesiophytes, or chrysophytes were actively growing in the water samples during the experiment, we created clonal libraries from intact rRNA purified from the samples with reverse transcriptase. The relationship between RNA content and growth rate has been well characterized for phytoplankton and bacteria (3, 9). A reconstructed phylogenetic tree for the 18S rRNA subunit is shown in Fig. 7. Comparison of gene phylogenies obtained for cloned *rbcL* and 18S sequences revealed several important similarities and discrepancies. The GRIST CH25 *rbcL* clone was found to be most similar (>92% at

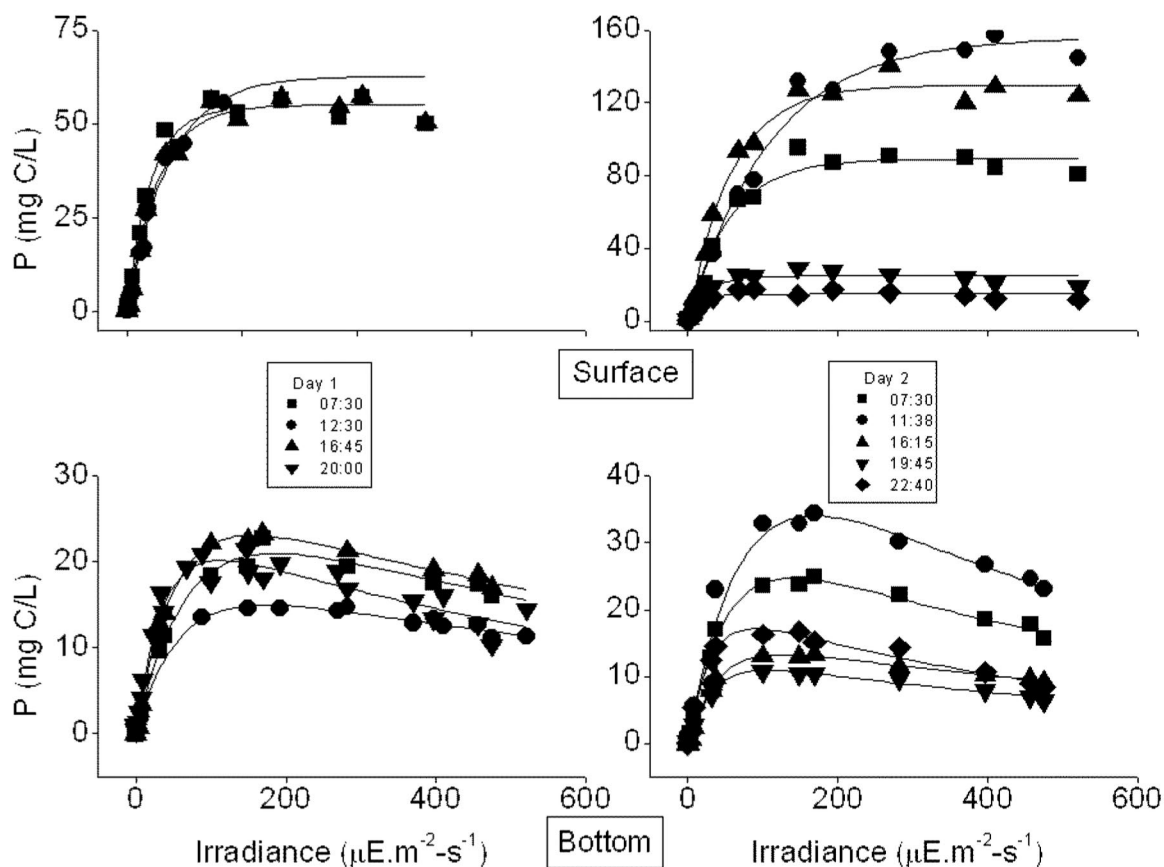


FIG. 3. Photosynthesis-irradiance curves for surface and bottom phytoplankton populations.

the amino acid level, Table 3) to *Detonula confervacea*, as demonstrated by phylogenetic analysis (Fig. 5). Similarly, the 18S clones G2D2T4 and C12D2T4 (Fig. 6) were found to be most closely related to *Detonula*. Two *rbcL* sequences were observed to be most similar to the diatom *Skeletonema costatum* (GRIST CH19 and CH27), but no corresponding 18S clones were observed. The GRIST CH29 clone was related to *Pedinella*, matching the B12D2T4 and G1D2T3 18S clones from both surface and deep samples. Sequences similar to a red alga, green algae, and one almost identical to *Bathycoccus prasinos* were not observed

among the sequence of the corresponding 18S library. Finally, the GRIST CH36 *rbcL* related to *E. huxleyi* was similar to the D1D2T3 18S clone. These results support the observation that diatoms and prymnesiophytes were actively photosynthesizing and growing during the experiment.

DISCUSSION

Finding molecular proxies that can distinguish and quantify biogeochemically active members in a microbial population

TABLE 2. Photosynthetic parameters of phytoplankton assemblages during the GRIST experiment

| Day | Time | Surface | | | | Deep | | | |
|-----|-------|---|--|--|-------|---|--|--|-------|
| | | α (mg of C/liter/ $\mu\text{E}/\text{m}^2$) | P^B_{max} (g of C/g of Chl a/liter) | β (mg of C/liter/ $\mu\text{E}/\text{m}^2$) | r^2 | α (mg of C/liter/ $\mu\text{E}/\text{m}^2$) | P^B_{max} (g of C/g of Chl g/liter) | β (mg of C/liter/ $\mu\text{E}/\text{m}^2$) | r^2 |
| 1 | 7:30 | 0.162 | 6.65 | 0 | 0.98 | 0.086 | 6.62 | 0.008 | 0.99 |
| | 12:30 | 0.091 | 6.55 | 0 | 0.99 | 0.078 | 4.86 | 0.005 | 0.99 |
| | 16:45 | 0.149 | 7.95 | 0 | 0.99 | 0.182 | 9.50 | 0.009 | 1.00 |
| | 20:00 | | | | | 0.182 | 6.73 | 0.009 | 0.96 |
| 2 | 7:30 | 0.077 | 4.24 | 0 | 0.98 | 0.118 | 6.07 | 0.008 | 0.99 |
| | 11:38 | 0.064 | 7.01 | 0 | 0.99 | 0.151 | 11.61 | 0.019 | 0.96 |
| | 16:15 | 0.075 | 4.32 | 0 | 0.99 | 0.098 | 4.01 | 0.005 | 1.00 |
| | 19:45 | 0.029 | 0.72 | 0 | 0.94 | 0.142 | 4.97 | 0.007 | 0.99 |
| | 22:40 | 0.064 | 1.09 | 0 | 0.92 | 0.251 | 7.58 | 0.014 | 0.99 |

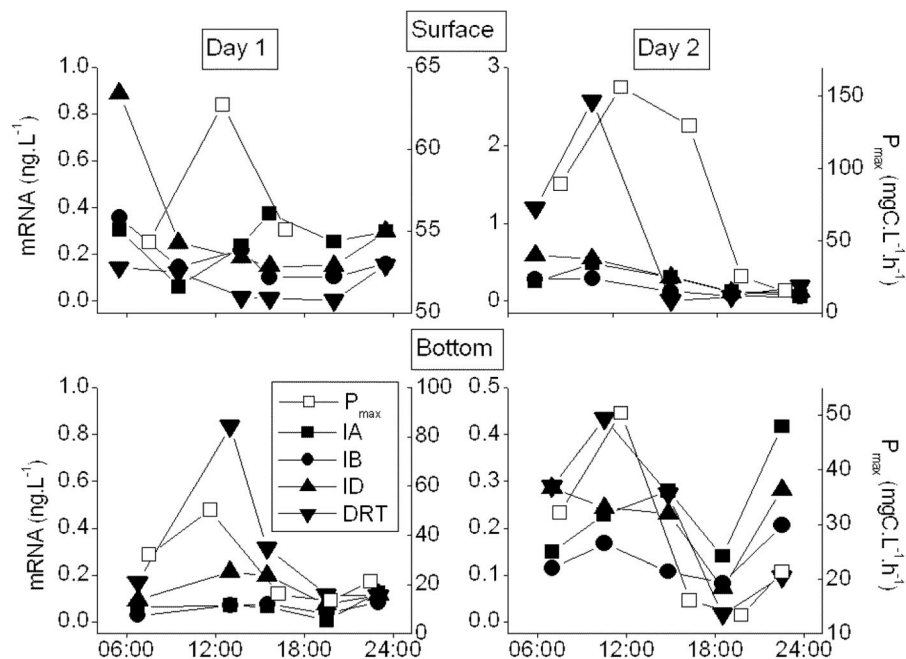


FIG. 4. Time course for *rbcL* mRNA abundance and light-saturated photosynthetic rate (P_{max}). IA, form IA *rbcL* mRNA; IB, form IB *rbcL* mRNA; ID, form ID *rbcL* mRNA; DRT, real-time diatom *rbcL* mRNA. Open squares, P_{max}^B . Right panels, day 1; left panels, day 2.

should provide a better understanding of how such populations respond to environmental parameters. Insight into the regulation and expression of photosynthetic processes is at the core of the global C cycle and is particularly pertinent to current environmental concerns. In this study, we sought to determine what photosynthetically active phytoplankton groups were present, the photosynthetic capacity of the assemblage, and the relationship of this activity to different sources of *rbcL* mRNA.

Diel variation of marine phytoplankton photosynthetic parameters has been well documented (11), and recent results indicate that such variability is in large part due to modulation of RubisCO transcription (19). The overriding factor in the regulation of RubisCO in vivo is light (3, 5, 14). Transcripts are

known to accumulate in the light and are degraded in the dark in a number of prokaryotic and eukaryotic algae. In the environment, *rbcL* transcription has been investigated in several studies (13, 16, 17, 19, 23, 24, 27). Mesocosm experiments and a Lagrangian study in the oligotrophic Gulf of Mexico revealed strong diel variation in form IB *rbcL* mRNA levels in surface waters, suggesting diel patterns in the regulation of *rbcL* transcription (19).

Form IB *rbcL* mRNA was significantly correlated with carbon fixation and was elevated during morning hours. In the water column, the highest cyano-*rbcL* transcripts (*Synechococcus* and *Prochlorococcus*) were observed at shallower depths, while chromo-*rbcL* transcripts were highest at the deep chlorophyll maximum, where chromophytic picoeukaryotes dominated, as determined by flow cytometry or epifluorescence microscopy (18). In addition to spatial segregation, a temporal separation in the peaks of chromo (form ID) and cyano (form IB) transcripts was also observed. Cyanobacterial *rbcL* transcript was predominantly found during morning hours, while chromophytic *rbcL* mRNA was most abundant in the late afternoon (16). However, both cyano *rbcL* mRNA and carbon fixation peaked in the early morning hours and were significantly correlated, suggesting that form IB *rbcL* mRNA was a good proxy for carbon fixation in these waters.

In contrast to the Gulf of Mexico and Tampa Bay studies, the Mid-Atlantic Bight (LEO 15) analysis of the transcriptionally active *rbcL* clones from a single time point indicated an abundance of chromophytic algae (a group that includes diatoms, prymnesiophytes, and chrysophytes), with a lesser amount of chlorophytic flagellates. These observations are in agreement with the accessory pigment analysis by HPLC and the major forms of *rbcL* mRNA encountered by probe hybrid-

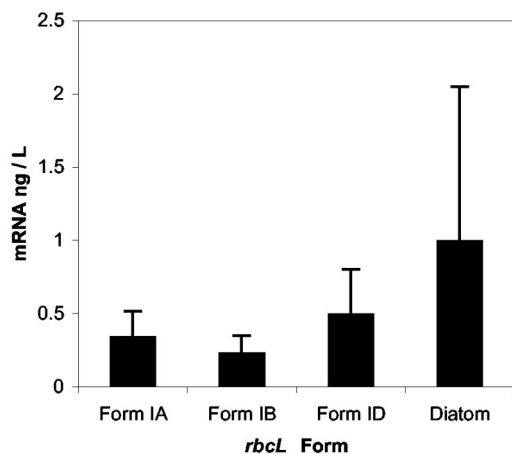


FIG. 5. Relative abundance of the different forms of *rbcL* mRNA observed during the experiment (averages of the daylight hours).

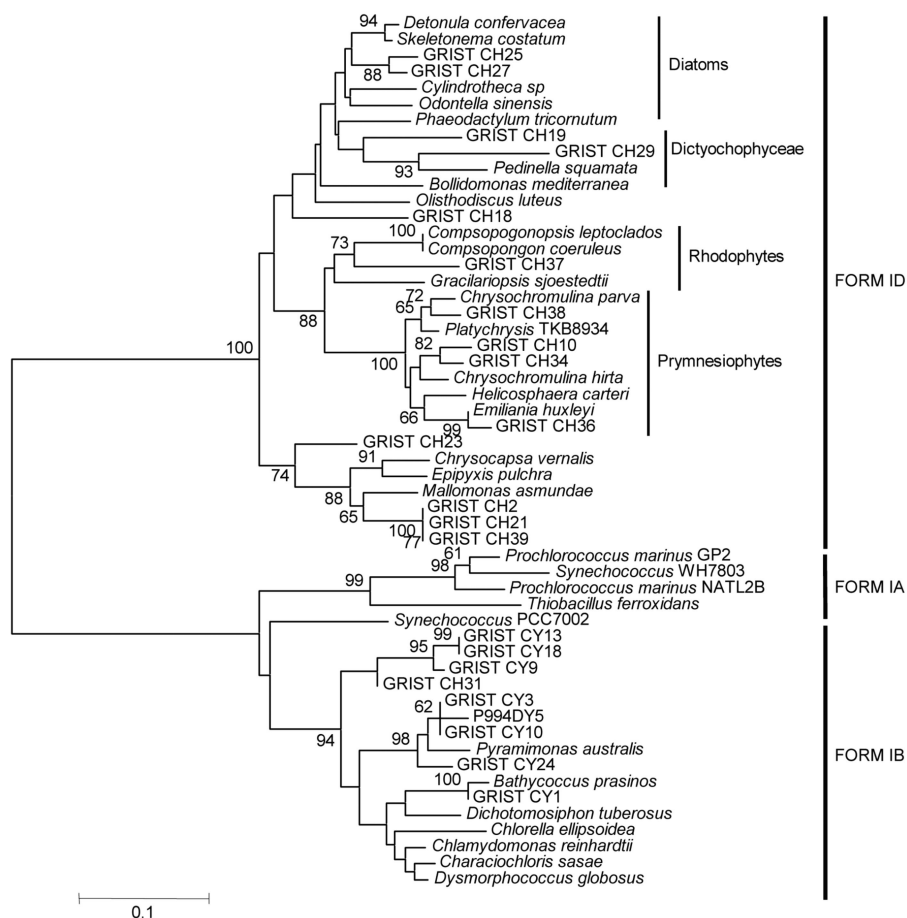


FIG. 6. Neighbor-joining tree of transcriptionally active *rbcL* clones obtained from the site (labeled GRIST and clone-specific suffix) and related sequences from GenBank. The clone labeled P994DY5 is from the Gulf of Mexico (25).

TABLE 3. Closest relatives of *rbcL* clones in GenBank

| Clone | Closest match in GenBank | % Amino acid identity |
|------------|-----------------------------------|-----------------------|
| GRIST CH10 | <i>Helicosphaera carteri</i> | 92 |
| GRIST CH18 | <i>Detonula confervacea</i> | 84 |
| GRIST CH19 | <i>Skeletonema costatum</i> | 90 |
| GRIST CH2 | <i>Mallomonas asmundae</i> | 91 |
| GRIST CH21 | <i>Mallomonas asmundae</i> | 91 |
| GRIST CH23 | <i>Skeletonema costatum</i> | 86 |
| GRIST CH25 | <i>Detonula confervacea</i> | 92 |
| GRIST CH27 | <i>Skeletonema costatum</i> | 92 |
| GRIST CH29 | <i>Pedinella sp. squamata</i> | 85 |
| GRIST CH31 | <i>Dysmorphococcus globosus</i> | 93 |
| GRIST CH34 | <i>Chrysochromulina hirta</i> | 94 |
| GRIST CH36 | <i>Emiliana huxleyi</i> | 98 |
| GRIST CH37 | <i>Gracilariopsis sjoestedtii</i> | 85 |
| GRIST CH38 | <i>Chrysochromulina parva</i> | 95 |
| GRIST CH39 | <i>Mallomonas asmundae</i> | 91 |
| GRIST CY1 | <i>Bathycoccus prasinus</i> | 98 |
| GRIST CY10 | <i>Pyramimonas australis</i> | 95 |
| GRIST CY13 | <i>Characiochloris sasae</i> | 90 |
| GRIST CY18 | <i>Characiochloris sasae</i> | 90 |
| GRIST CY24 | <i>Pyramimonas australis</i> | 94 |
| GRIST CY3 | Uncultured chlorophyte P994DY5 | 97 |
| GRIST CY9 | <i>Chlamydomonas reinhardtii</i> | 91 |

ization (i.e., form ID and diatom-specific *rbcL* mRNA; Fig. 4 and 5). This was also supported by the analysis of 18S rRNA clone libraries, which yielded sequences of similar phylogenetic affinity (in certain instances) as our *rbcL* clone libraries. It was also interesting to note the absence of oligotrophic oceanic picoplankton such as *Synechococcus* and *Prochlorococcus* in our *rbcL* clone libraries.

HPLC analysis of GRIST samples revealed predominance of pigments associated with chromophytes (fucoxanthin) and chlorophytes (chlorophyll *b*). Minor occurrences of peridinin and the absence of 19' butanoyloxyfucoxanthin and 19' hexanoyloxyfucoxanthin indicated predominance of diatoms relative to dinoflagellates and absence of prymnesiophytes and chrysophytes. The high proportions of fucoxanthin and chlorophyll *b* are indicative of a phytoplankton assemblage dominated by chromophytes and chlorophytes, while the low concentrations of zeaxanthin indicated lesser numbers of cyanophytes (Fig. 8). Thus, diatoms and chlorophytes appear to have been the predominant carbon-fixing components of the phytoplankton at the time of our experiment based on all assays: probe hybridization (*rbcL* mRNA), clonal analysis by RT-PCR (*rbcL* and 18S rRNA genes), and biochemical (HPLC) analyses.

The relationship between *rbcL* mRNA and P_{max} during the

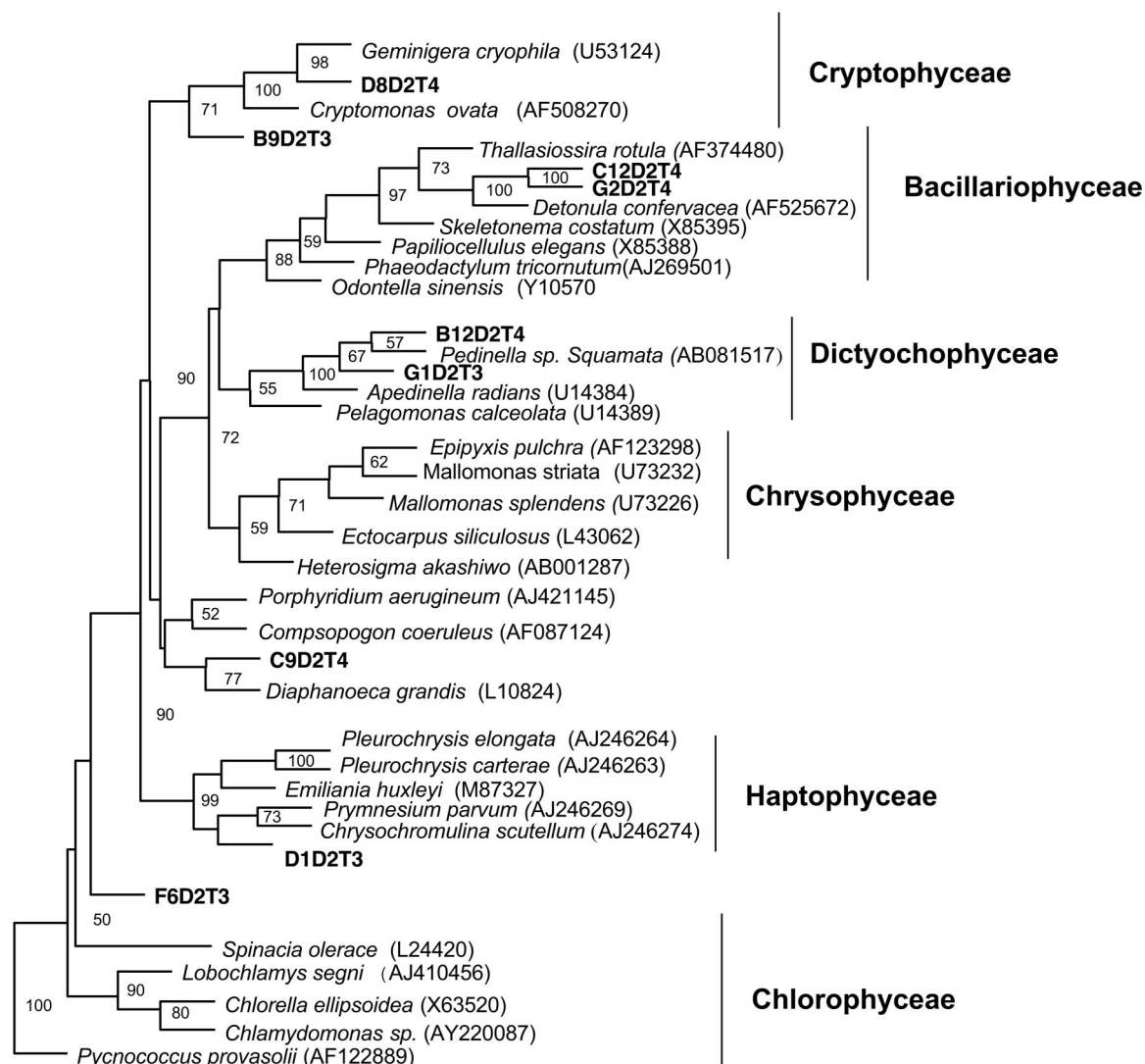


FIG. 7. Phylogenetic tree based on 18S rRNA genes obtained via reverse transcription of intact ribosomes during GRIST with maximum-likelihood methods.

GRIST experiment may have been affected by environmental variability as advection of water masses with different physical properties (Fig. 1) may have resulted in the replacement of phytoplankton populations. Large changes in pigment composition associated with an increase in thermocline intensity suggest a population shift in surface waters during the morning of day 1 (Fig. 8). However, afternoon increases in diatom dominance as reflected in fucoxanthin concentrations did not correspond to peaks in diatom or form ID mRNA in three of four diel samples, suggesting that the transcriptional signal overshadowed the changes in community composition or in situ pigment synthesis. Total mRNA yields (total mRNA was quantified in all samples prior to dotting; data not shown) exhibited good correlations with pigment levels, particularly to chlorophyll c_1 , fucoxanthin and zeaxanthin ($R^2 = 0.68, 0.57,$ and 0.77 , respectively; $P < 0.001$ for all three), but were not significantly correlated with the individual mRNA signals (form IA: $P = 0.38$; IB: $P = 0.17$; ID: $P = 0.29$; diatom: $P = 0.627$). This

indicates that variations in *rbcL* mRNA levels were not caused by population level-dependent changes of total mRNA, but were caused by transcriptional regulation of phytoplankton *rbcL* mRNA.

Correlation between *rbcL* mRNA and P_{\max} is, as expected, dependent on the particular type of *rbcL* mRNA examined (Fig. 9), the most robust correlation ($R^2 = 0.56$) corresponding to type ID *rbcL* mRNA ($R^2 = 0.56$) and the least robust ($R^2 = 0.41$) corresponding to type IA. Overall, correlation between *rbcL* hybridization data and photosynthetic carbon fixation was statistically significant at $R^2 = 0.58$ ($P = 0.00064$). Real-time diatom *rbcL* mRNA correlated moderately with P_{\max} ($R^2 = 0.49$; $n = 12$). However, two afternoon (3:40 p.m. on day 1 and 4:20 p.m. on day 2) surface samples showed barely detectable levels of diatom *rbcL* mRNA despite the high photosynthetic capacity observed at these times. We attribute this to mRNA degradation in the presence of high levels of functional RubisCO protein. Removal of the two data points yields a

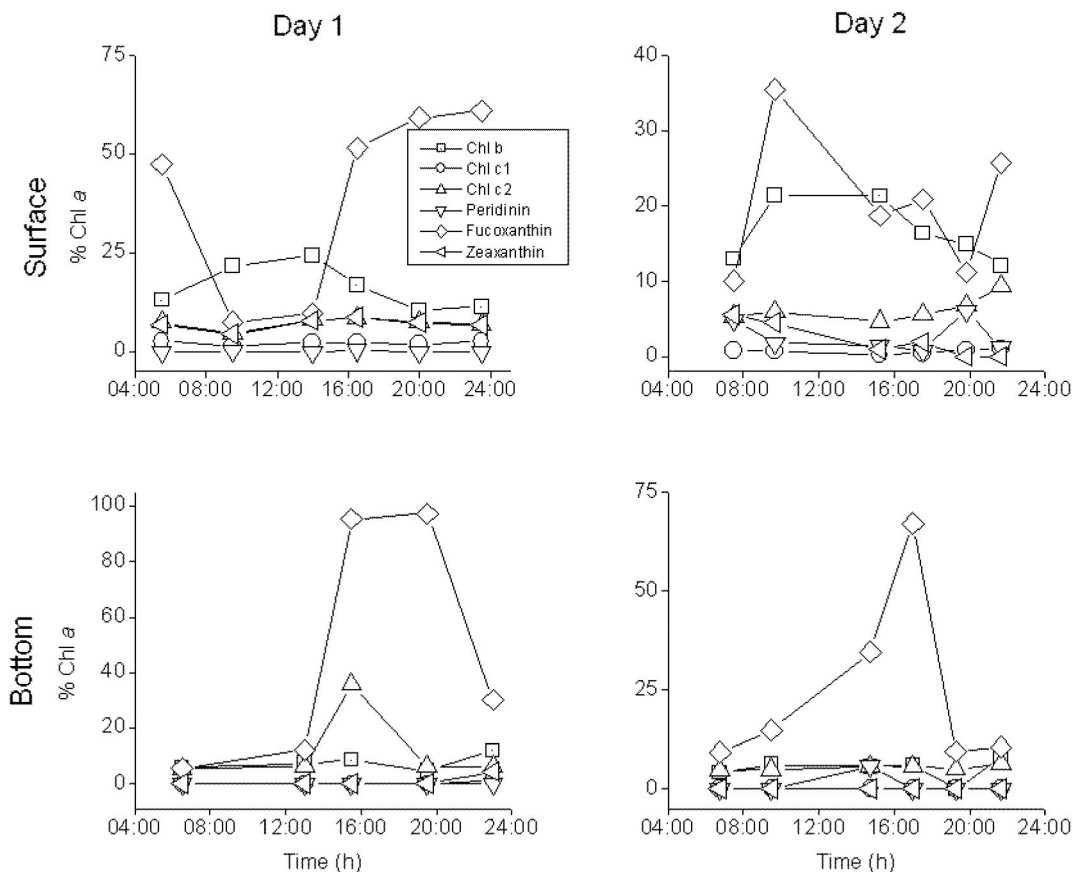


FIG. 8. Relative abundance of photosynthetic pigments as a percentage of chlorophyll *a* content.

remarkably tight correlation ($R^2 = 0.97$ $n = 10$) indicating close coupling between gene transcription and photosynthetic rate (Fig. 10) for most of the day.

Our results suggest that transcriptional regulation may have been important for certain time series (day 2) of the GRIST experiment after initial bloom development. Correlations between *rbcL* mRNA and P_{max} were low during day 1, but biomass and photosynthetic rate variability were modest at this time. Closer correlations were observed on day 2 when light-saturated photosynthetic rates varied over one order of magnitude (13 to 160 mg of C liter⁻¹ h⁻¹). Late-night increases in both mRNA abundance and photosynthetic capacity of the deep-water assemblage constitute a novel observation.

Although transcription has been used to some degree as a surrogate for gene expression, uncertainty remains regarding the predictability of biogeochemical activity based upon transcript abundance alone. Enzymes are subject to a host of post-transcriptional controls and RubisCO control is complex, particularly in eukaryotes. Several mechanisms for metabolic regulation of RubisCO activity are known (5). These include reversible activation of the active site by CO₂, binding of non-competitive inhibitors to the active site and binding of effectors at sites other than the active site. In general, these controls respond to the relative abundance of RubisCO substrates and to NADP/NADPH and ADP/ATP ratios. Posttranscriptional mechanisms of regulation are active in eukaryotes (13), but

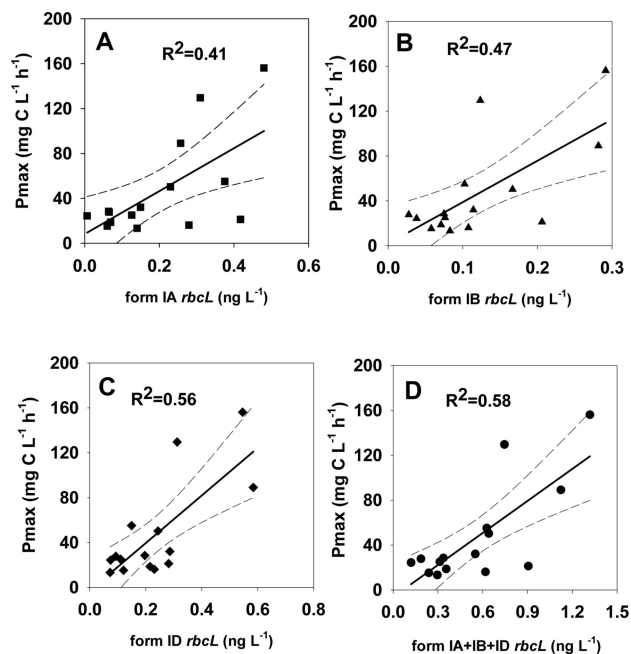


FIG. 9. Relationship between PCR *rbcL* mRNA abundance and light-saturated photosynthetic rate. The linear relationship is given by $y = -6 + 95.5x$ ($r^2 = 0.58$; $n = 16$).

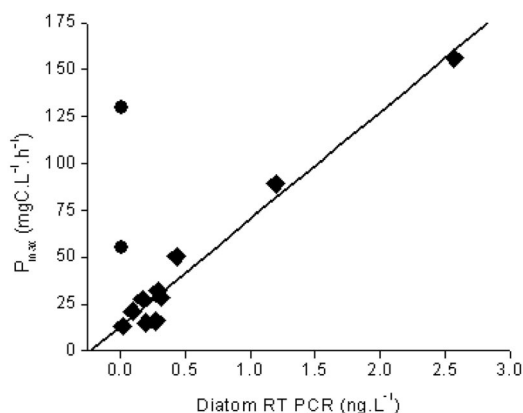


FIG. 10. Relationship between real-time PCR diatom *rbcL* mRNA abundance and light-saturated photosynthetic rate. The linear relationship, excluding the outliers marked in gray, is given by $y = 13.2 + 57.1x$ ($r^2 = 0.97$; $n = 10$).

transcriptional regulation appears to be the overriding factor in the regulation of carbon fixation in cyanobacteria (15, 22).

In summary, a strong relationship between photosynthetic capacity and transcription of the *rbcL* gene by diatoms was observed in three of four diel time series at the LEO 15 site off Tuckerton, N.J. This implies that transcriptional regulation of *rbcL* genes can be a major factor controlling carbon fixation in this coastal environment.

ACKNOWLEDGMENTS

GRIST was carried out under the auspices of the U.S. Department of Energy Biotechnological Investigations Ocean Margin Program (BIOMP; grants DE-FG02-00ER62978 to L.K. and J.E.C. and DE-FG02-97ER62452 to J.H.P.).

We thank Lora McGuinness for sample collection and logistics, Alvaro Cabrera for assistance in the photosynthetron incubations, Ana Lozada for analysis of chlorophyll *a*, particulate organic C, and particulate organic N, and the crew of the RVs *Arabella* and *Caletta* for sample collection and transport.

REFERENCES

- Altschul, S. F., T. L. Madden, A. A. Schaffer, J. Zhang, Z. Zhang, W. Miller, and D. J. Lipman. 1997. Gapped BLAST and PSI-BLAST: a new generation of protein database search programs. *Nucleic Acids Res.* **25**:3389–3402.
- Côté, B., and T. Platt. 1983. Day-to-day variations in the spring-summer photosynthetic parameters of coastal marine phytoplankton. *Limnol. Oceanogr.* **28**:320–344.
- Dortch, Q., T. L. Roberts, J. J. R. Clayton, and S. I. Ahmed. 1983. RNA/DNA ratios and DNA concentrations as indicators of growth rate and biomass in planktonic marine organisms. *Mar. Ecol. Prog. Ser.* **13**:61–71.
- Glenn, S. M., M. F. Crowley, D. B. Haidvogel, and Y. T. Song. 1996. Underwater observatory captures coastal upwelling events of New Jersey. *Eos Trans. Am. Geophys. Union* **77**:233–236.
- Hartman, F. C., and M. R. Harpel. 1994. Structure, function, regulation, and assembly of D-ribulose-1,5-bisphosphate carboxylase/oxygenase. *Annu. Rev. Biochem.* **63**:197–234.
- Kerkhof, L., J. Corredor, J. Paul, D. Bronk, J. Lopez, and J. Cherrier. 2003. Experiment explores intercalibration of biogeochemical flux and nucleic acid measurements. *Eos Trans. Am. Geophys. Union* **84**:167.
- Kerkhof, L., and P. Kemp. 1999. Small ribosomal RNA content in marine proteobacteria during non-steady-state growth. *FEMS Microbiol. Ecol.* **30**:253–260.
- Kerkhof, L., M. Santoro, and J. Garland. 2000. Response of soybean rhizosphere communities to human hygiene water addition as determined by community-level physiological profiling (CLPP) and terminal restriction fragment length polymorphism (TRFLP) analysis. *FEMS Microbiol. Lett.* **194**:95–101.
- Kerkhof, L., and B. B. Ward. 1993. Comparison of nucleic acid hybridization and fluorometry for measurement of the relationship between RNA/DNA ratio and growth rate in a marine bacterium. *Appl. Environ. Microbiol.* **59**:1303–1309.
- Kumar, S., K. Tamura, and M. Nei. 1993. MEGA: molecular evolutionary genetic analysis, version 2.0. The Pennsylvania State University, University Park.
- MacCaul, W., and T. Platt. 1977. Diel variations in the photosynthetic parameters of coastal marine phytoplankton. *Limnol. Oceanogr.* **22**:723–731.
- Paul, J. H. 2001. *Marine microbiology*, vol. 30. Dowden, Hutchinson & Ross, New York, N.Y.
- Paul, J. H., A. Alfreider, J. B. Kang, R. A. Stokes, D. Griffin, L. Campbell, and E. Ornlodottir. 2000. Form IA *rbcL* transcripts associated with a low salinity/high chlorophyll plume ('Green River') in the eastern Gulf of Mexico. *Mar. Ecol. Prog. Ser.* **198**:1–8.
- Paul, J. H., A. Alfreider, and B. Wawrik. 2000. Micro- and macrodiversity in *rbcL* sequences in ambient phytoplankton populations from southeastern Gulf of Mexico. *Mar. Ecol. Prog. Ser.* **198**:9–18.
- Paul, J. H., J. B. Kang, and F. R. Tabita. 2000. Diel patterns of regulation of *rbcL* transcription in a cyanobacterium and a prymnesiophyte. *Mar. Biotechnol.* **2**:429–436.
- Paul, J. H., S. L. Pichard, J. B. Kang, G. M. F. Watson, and F. R. Tabita. 1999. Evidence for a clade-specific temporal and spatial separation in ribulose biphosphate carboxylase gene expression in phytoplankton populations off Cape Hatteras and Bermuda. *Limnol. Oceanogr.* **44**:12–23.
- Pichard, S., M. E. Frisher, and J. H. Paul. 1993. Ribulose biphosphate carboxylase gene expression in subtropical marine phytoplankton populations. *Mar. Ecol. Prog. Ser.* **101**:55–65.
- Pichard, S. L., L. Campbell, K. Carder, J. B. Kang, J. Patch, F. R. Tabita, and J. H. Paul. 1997. Analysis of ribulose biphosphate carboxylase gene expression in natural phytoplankton populations by group-specific gene probing. *Mar. Ecol. Prog. Ser.* **149**:239–253.
- Pichard, S. L., L. Campbell, J. B. Kang, F. R. Tabita, and J. H. Paul. 1996. Regulation of ribulose biphosphate carboxylase gene expression in natural phytoplankton communities. I. Diel rhythms. *Mar. Ecol. Prog. Ser.* **139**:257–265.
- Platt, T., S. Sathyendranath, and P. Ravindran. 1990. Primary production by phytoplankton: analytic solutions for daily rates per unit area of water surface. *Proc. R. Soc. Lond. Ser. B* **241**:201–211.
- Tabita, F. R. 1988. Molecular and cellular regulation of autotrophic carbon dioxide fixation in microorganisms. *Microbiol. Rev.* **52**:155–189.
- Watson, G. M., and F. R. Tabita. 1996. Regulation, unique gene organization, and unusual primary structure of carbon fixation genes from a marine phycoerythrin-containing cyanobacterium. *Plant Mol. Biol.* **32**:1103–1115.
- Wawrik, B., J. H. Paul, L. Campbell, D. Griffin, L. Houchin, A. Fuentes-Ortega, and F. Mueller-Karger. 2003. Vertical structure of *rbcL*-containing phytoplankton phylotypes associated with a coastal plume in the Gulf of Mexico. *Mar. Ecol. Prog. Ser.* **251**:87–101.
- Wawrik, B., J. H. Paul, and F. R. Tabita. 2002. Real-time PCR quantification of *rbcL* (ribulose-1,5-bisphosphate carboxylase/oxygenase) mRNA in diatoms and pelagophytes. *Appl. Environ. Microbiol.* **68**:3771–3779.
- Welschmeyer, N. A. 1994. Fluorometric analysis of chlorophyll *a* in the presence of chlorophyll *b* and pheopigments. *Limnol. Oceanogr.* **39**:1985–1992.
- Wright, S. W., and S. W. Jeffrey. 1997. High-resolution HPLC system for chlorophylls and carotenoids of marine phytoplankton, p. 343–360. *In* S. W. Jeffrey, R. F. C. Mantoura, and S. W. Wright (ed.), *Phytoplankton pigments in oceanography*. UNESCO, Paris, France.
- Wyman, J., J. P. Zehr, and D. G. Capone. 1996. Temporal variability in nitrogenase gene expression in natural populations of the marine cyanobacterium *Trichodesmium thiebautii*. *Appl. Environ. Microbiol.* **62**:1073–1075.